Bulgarian Chemical Communications, Volume 55, Special Issue A (pp. 225-231) 2023 DOI: 10.34049/bcc.55.A.0034

Thermal kinetics of poly(amidoamine) functionalized silica gel

V. K. Singh[1*], M. Musharraf[1], S K Swain[2], R K Dey[3], S. Shekhar[4*]

[1]*Department of Chemistry, Teerthanker Mahaveer University, Moradabad, Uttar Pradesh-244001, India*
[2] *Central Instrumentation Facility, Birla Institute of Technology, Mesra, Ranchi, Jharkhand-835215, India*
[3]*Department of Chemistry, Central University of Jharkhand, Ranchi, Jharkhand-835205, India*
[4]*Daudnagar College, Daudnagar (Aurangabad), Magadh University, Bodhgaya, Bihar-824113, India*

Received: April 7, 2023; Revised August 02, 2023

In the present work, the degradation steps of polyamidoamine (PAA) functionalized silica gel (SiPOLHOM) was investigated under dynamic conditions. The degradation of SiPOLHOM was studied with thermogravimetric analyzer (TGA). The kinetics of degradation process was analyzed by Kissinger method, Flynn–Wall–Ozawa's (FWO) method and deconvolution method. The degradation of SiPOLHOM was explained by two-portion process model (PI-TPPM), according to which the decomposition of PAA moieties takes place in two steps called process 1 and 2. Also, Flynn–Wall–Ozawa's (FWO) method and deconvolution method were used to evaluate the apparent activation energy (Ea).

Keywords: Poly (amido amine), Silica gel, Activation energy, Kinetic triplet, Deconvolution method

INTRODUCTION

Chemically modified silica gels have been paid much attention for adsorption process and other applications [1-6]. Such applications require assessment of thermal properties to understand their structural integrity, functional performance and overall suitability for specific needs. The study of thermal stability is also very crucial while designing materials for high-temperature applications such as adsorption, catalyst supports, thermal barrier coatings and gas separation membranes [7-9]. In the quest for understanding and plan the applications of chemically modified silica gels, the knowledge of thermal decomposition under different conditions may be helpful [10-14]. It enables researchers and engineers to optimize material synthesis with improved process efficiency and enhanced thermal properties. There currently exist many literatures available on degradation kinetics of polymers and composites using different conditions and kinetic models [15-20].

Degradation kinetics of chemically modified silica gels is affected by various factors so it is difficult to reveal their mechanism of decomposition [21-28]. Thermal decomposition generally consists of different steps, and it is challenging to predict a global mechanism to formulate the degradation kinetics. Therefore, some well-known methods were used to study the thermal degradation kinetics. Valuable information regarding characteristics of thermal degradation, i.e., the mechanism of degradation reaction, kinetic triplet, thermal stability and phase change, can be determined from thermogravimetric analysis (TGA) or differential thermogravimetric (DTG) curves [18, 29]. The kinetic triplet (i.e., E, A, and f(a)-function) offer mathematical description which can be used to generate the parent kinetic data as well as to predict the degradation kinetics beyond the range of experimental temperature [30]. The results of kinetic study can be applicable for development of composite material in industrial purpose [31].

The main goal of present work is to analyze the thermal degradation kinetic of chemically modified silica and evaluate the kinetics triplet using thermogravimetric data. Also, the present work is targeted to reveal the devolatilization kinetics during thermal decomposition of chemically modified silica gels, under dynamic circumstances at different heating rates.

In this context, the present work reveals the investigation results related to thermal analysis of polyamidoamine (PAA) immobilized silica gel. The detailed report on characterization of material & its metal binding behaviors are explored in our earlier work [32].

MATERIALS AND METHODS

Starting materials

All reagents: piperazine (Aldrich), 3-chloropropyltrimethoxysilane (Aldrich) and methylene-bis-acrylamide (Acros) were used without purification. Silica gel (0.063–0.200 mm particle size, 60 Å pore diameter, 2.82 g mL^{-1}

* To whom all correspondence should be sent:
E-mail: vks2679@gmail.com,
ss_chem85@rediffmail.com

pore volume, 422 m^2g^{-1} surface area) was purchased from Fluka. An ultra-pure Milli-Q 18.2 MV system was used to produce doubly distilled water (DDW).

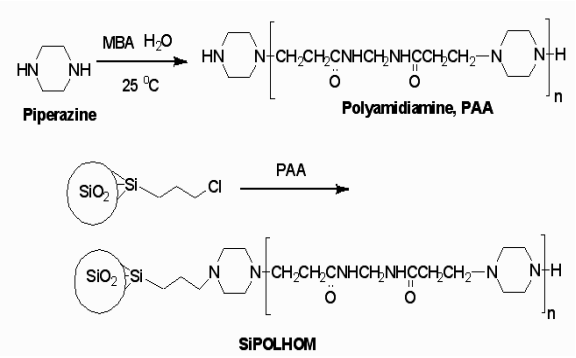

Scheme 1. Synthetic route of poly (amido amine) functionalized silica surface

Material synthesis

The fictionalization of silica surface was done as process adopted by Dey *et al.* [32]. Firstly, preparation of polyamidoamines (PAAs) was done *via* mixing 7.5 g of MBA with 4.4 g of piperazine in deionized water. The resulting suspension was stirred slowly at room temperature for seventy-two hours. Once PAA formed, 2.1 g of organo-functionalized silica (SiCl) was mixed with it. After that 2.0 mL of triethylamine was added to it & the stirring continued for 50 hours at a temperature of 60ºC. The final material SiPOLHOM was filtered, washed with ethanol and dried in vacuum.

Thermal study

The thermogravimetric analysis (TGA) and differential scanning calorimetry (DSC) of the samples were carried out on a TA Instruments, USA;Q10 in argon atmosphere with flow rate of 30 cm^3 s^{-1}, in the range of temperature from room temperature to 1000 °C at the heating rate of 5, 10, 15, 20°C/min, respectively.

Calculation procedure

Thermogravimetric (TG) analysis was used to determine degradation kinetics which can be described with various equations describing degradation mechanisms [18]. The rate of reactions involved during degradation analyzed as a function of the temperature T, and degree of conversion x, which is calculated by:

$$x = \frac{W_0 - W_t}{W_0 - W_f} \quad (1)$$

where W_0 – weight of sample (gm), W_t – weight of sample at time t, W_f – Final weight of sample.

During degradation the rate of decomposition $\left(\frac{dx}{dt}\right)$ is a function of temperature and weight of the sample while the rate of conversion (x) is assumed to be proportional to the concentration of the sample. Then, the rate of conversion (x) can be given:

$$\frac{dx}{dt} = k(T).f(x) \quad (2)$$

The apparent activation energy (E_a) may be expressed as the following equation for non-Arrhenius type temperature dependence of reactions,

$$E_a = RT^2.\frac{dlnk}{dT} = -R.\frac{d\ ln\ k}{d\left(\frac{1}{T}\right)} \quad (3)$$

leading to Arrhenius equation:

$$k(T) = A.e^{-E_a/RT}.$$

where k(T) represents the rate constant, R denotes the gas constant, and "A" refers to pre-exponential factor [27].

For non-isothermal degradation process linear heating rate H=dT / dt is used to change the variable from time (t) into the temperature (T),

$$H.\left(\frac{dx}{dT}\right) \equiv \left(\frac{dx}{dt}\right) = k(T).f(x) = A.e^{-E_a/RT}.(1-x)^n \quad (4)$$

Kissinger method

Kissinger method is also called model free method used to determine the kinetic triplet and E_a without knowing the reaction pathway [33]. We can evaluate the E_a using Eq. (4).:

$$ln\left(\frac{H}{T_p^2}\right) \equiv \left(\frac{dx}{dt}\right) = ln\left\{\left(\frac{A.R}{E_a}\right).[-f'_x(x)]\right\}.^{-E_a/RT} \quad (5)$$

where T_p represents the peak temperature. E_a can be calculated from the slope of the plot of $\ln(H/T_p^2)$ verses $1/T_p$. In the present case, $f'_x(x) = -1$ (for first order kinetics) in Eq. (5). In addition, the preexponential factor (A) for degradation process in the case of n^{th} order (when $n \neq 1$), may be calculated based on following equation:

$$A \approx H \cdot A.\exp\left(\frac{E_a}{RT_p}\right)/RT_p^2$$

FWO method

Flynn–Wall–Ozawa's (FWO) integral isoconversional method is the most commonly used method [34-36] which can be represented as follows:

$$ln\ H = \ln[constant.A] - 1.052.\frac{E_a}{RT_p} \quad (6)$$

ln H was plotted against 1/T, at different heating rates, for the similar value of x considered within 5–95% limits as given in Eq. (6), can be used to calculate E_a. The slope of the plot is utilized to

evaluate the activation energy (slope=−1.052 · (E_a / R)).

Deconvolution method

Linear algorithm model of deconvolution has been applied to extract each process of decomposition rate signal. On the basis of superposition principle, the recorded rate signal is always equal to the signal of every component in its participation proportion (Eq. 7) [29]:

$$\left(\frac{dx}{dT}\right) = \sum_{i=1}^{p} C_i \frac{dx_i}{dt} \quad (7)$$

where C_1, C_2, …, C_p represents constants as weight values and p denotes the number of processes. Applying superposition principle for individual process Eq. (4), can be written as following [29]:

$$\frac{dx}{dt} = \sum_{i=1}^{p} C_i . A_i e^{-E_{a,i}/RT} . (1-x)^{n_i} \quad (8)$$

where E_{ai} represents the apparent activation energy of each process "i", which can be approximated graphically with a Gaussian curve in the following form [29]:

$$\frac{dx_i}{dx} = \frac{1}{\sqrt{2\pi\sigma_i}} . exp\left[-\frac{1}{2} . \frac{(T-T_p)^2}{\sigma_i}\right] \quad (9)$$

where T and T_p represent the independent variable and peak location on the rate curve, respectively, σ_i denotes standard deviation. As a result, assuming linear sum of Gaussian curves approximates whole conversion in thermal decomposition is given as follows:

$$\frac{dx}{dt} = \sum_{i=1}^{p} C_i . \frac{1}{\sqrt{2\pi}} . \frac{1}{\sigma_i} . exp\left[-\frac{1}{2} . \frac{(T-T_p)^2}{\sigma_i}\right] \quad (10)$$

where $C_i . \frac{1}{\sqrt{2\pi\sigma_i}}$ denotes the area of fitted peak.

RESULTS AND DISCUSSION

Thermal degradation

The thermal degradation of SiPOLHOM is shown in Figure 1. It can be observed that material degrade in multiple stages. In the first stage mass loss up to 100°C may be attributed to loss of moisture in the material. In next stage, it can be seen a small weigh down part on the TG graph where weight loss continues up to 600°C due to degradation of PAA chain attached to silica surface. The degradation pattern shown in figure indicates that PAA degrades in multiple scissions. PAA degradation takes place mainly in two regions first from 220-310°C and 2nd from 315-597°C. After 600°C the mass loss rate decreases.

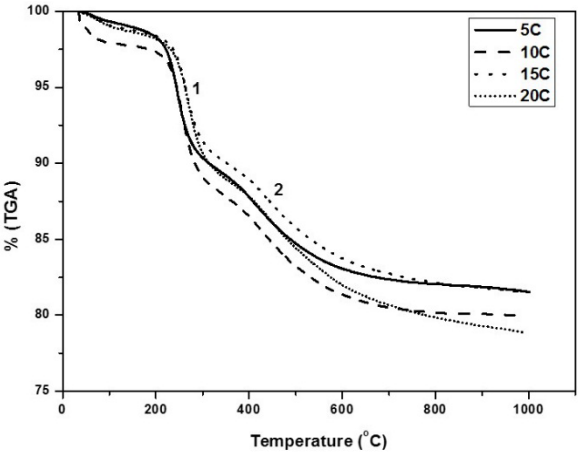

Figure 1. TG curve of SiPOLHOM

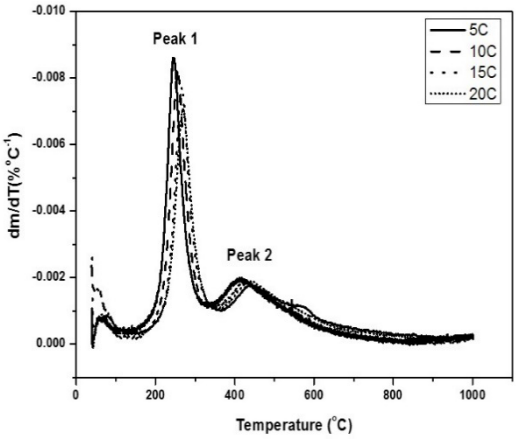

Figure2. DTG curve of SiPOLHOM

The TG and DTG curves of silica supported by PAA obtained at the heating rate of 5, 10, 15 and 20°C are shown in Figures 1 and 2, respectively. The major degradation takes place in the first region ("1") where the majority of PAA was lost. Such region is called an active degradation zone, as major part of PAA decomposed in a sequence manner. In the second region ("2") the rest compound partially decomposed termed as slow decomposition stage.

Figures 1 and 2 refer to process 1 and process 2, respectively. Figure 2 depicts the DTG curve of SiPOLHOM showing two distinct peaks (marked as peak 1 and peak 2) between 200 and 600 °C. The first peak found between 200–320 °C which can be assigned to the sequenced decomposition of main chain of PAA. The second peak positioned between 340–600°C is due to decomposition of remaining organic part of SiPOLHOM. It can be pointed out that the small peaks become distinct when the rate of heating increased.

Kinetic analysis

Kissinger method

The Kissinger plots obtained using T_p for all processes are depicted in Figure 3 and their kinetics results are presented in Table 1. The value of apparent activation energy (Ea) and pre-exponential factor (A) (Table 1) are found to be different for each process due to the difference in energy required for the decomposition of main chain of PAA (p = 1) and remaining organic part of SiPOLHOM. (p = 2), respectively.

Table 1. Results estimated from the Kissinger method for SiPOLHOM.

Kissinger (peak) analysis	$\ln(H/T_p^2)$ vs. $1/T_p$	
	Process 1	Process 2
E_a (kJ mol^{-1})	4.416	5.660
lnA	-1.62	-1.90
A (min^{-1})	0.197	0.149
RSS	0.00151	0.00135

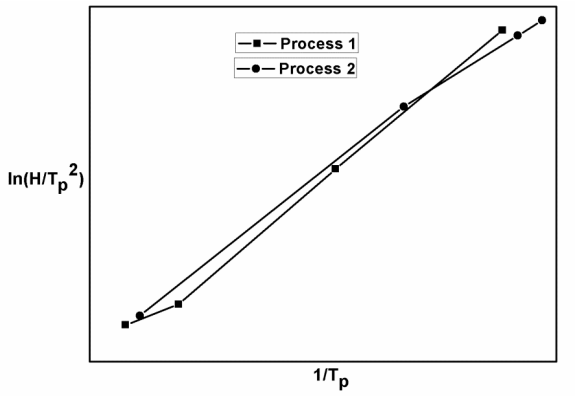

Figure 3. Kissinger plot of SiPOLHOM

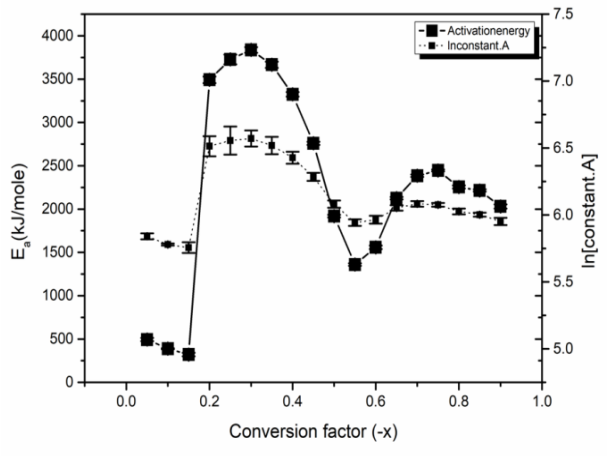

Figure 4. FWO plot of SiPOLHOM

FWO method

The apparent activation energies determined using FWO method are depicted in Figure 4. This provides information about $E_a = E_a(x)$ and iso-conversional intercept (ln [constant · A]) dependency on the fraction of conversion. It is observed that the on the whole decomposition process executed in multi-steps decomposition reactions in which each step reaction contributes partially to the whole reaction mechanism to a dissimilar extent, depending on the process of decomposition [29]. Similar trends were found in case of in E_a and iso-conversional intercept.

The E_a decreased steeply from 493 to 320.9 kJ mol^{-1} between 0.05 and 0.15 of x then it increased up to 3837 kJ mol^{-1} between 0.2 and 0.3 of x. It again found to be decreased to 1359 kJ mol^{-1} in the intervals of x = 0.30–0.55 followed by an increment up to 2445kJ mol^{-1}in the interval of x=0.60-0.75. However, the value of E_a is found to be stable when the value of x lies between 0.75 and 0.90. E_a exhibits lower value at the initial decomposition stage up to x = 0.15, which attributes to loss of water vapor [37]. The major change in E_a when conversion fraction lies between 0.2 and 0.3 for temperature range 200-320°C, may be attributed to major degradation of PAA chain in region ("1") results into peak 1 (Figure 2). The E_a value increased from 1359 kJ mol^{-1} to 2445kJ mol^{-1} when the conversion fraction increased from 0.55 to 0.75, and beyond 0.75, E_a started to decrease (Fig. 5). The changes in the value of E_a happen above 322°C, in region ("2") including peak 2 (Figure 2).

Deconvolution analysis and kinetic parameters

Deconvolution method was applied to separate the individual process of degradation using Gaussian algorithm to rate curves at different heating rates 5, 10, 15 and 20°C min^{-1}, depicted in Figure 5 showing two Gaussian curves corresponding to two core processes. Two peaks, p, have been found except at higher heating rate 20°C min^{-1} where a small peak observed around 80°C. The Gaussian function points of linear combination required value close to the experimental data in rate curve for performing linear deconvolution algorithm.

Gauss curves corresponding to studied processes

The results of the deconvolution method are depicted in Table 2 showing quality of fitting. The heating rate is found to affect the magnitudes of area of each fitted peak ($C_i \cdot [1 / (2\pi)1/2 \cdot \sigma_i]$), T_p and standard deviation (σ_i, FWHM), for process 1 and process 2 (Figure 5). Also, it is observed that a small peak appears on increase in rate of heating, 20°C min^{-1}. The degradation rate has been found continuously increased on increasing the rate of

heating of process 1 and process 2 as per result presented in Table 2.

Differential scanning calorimetry

The DSC signatures for SiPOLHOM at the four varied rate of heating can be seen in the curves of Figure 6 with the accompanying data in Table 1. It seems that the heating rate have much effect on the degradation of SiPOLHOM. The temperature at the peak of mass loss occurred at 341°C, 428°C, 482°C, 480°C at the heating rate of 5, 10, 15, 20°C/minute, respectively, which may be attributed to the removal of the organic moieties. We found a slow and continuous mass loss in the second peak of each curve observed at 673 °C, 754 °C, 803 °C and 801°C with the heating rate of 5, 10, 15, 20°C/minute, respectively. It is due to silanol condensation to stable siloxane, Si–O–Si bonds. The peak of the temperature was found to increase with increase in rate of heating.

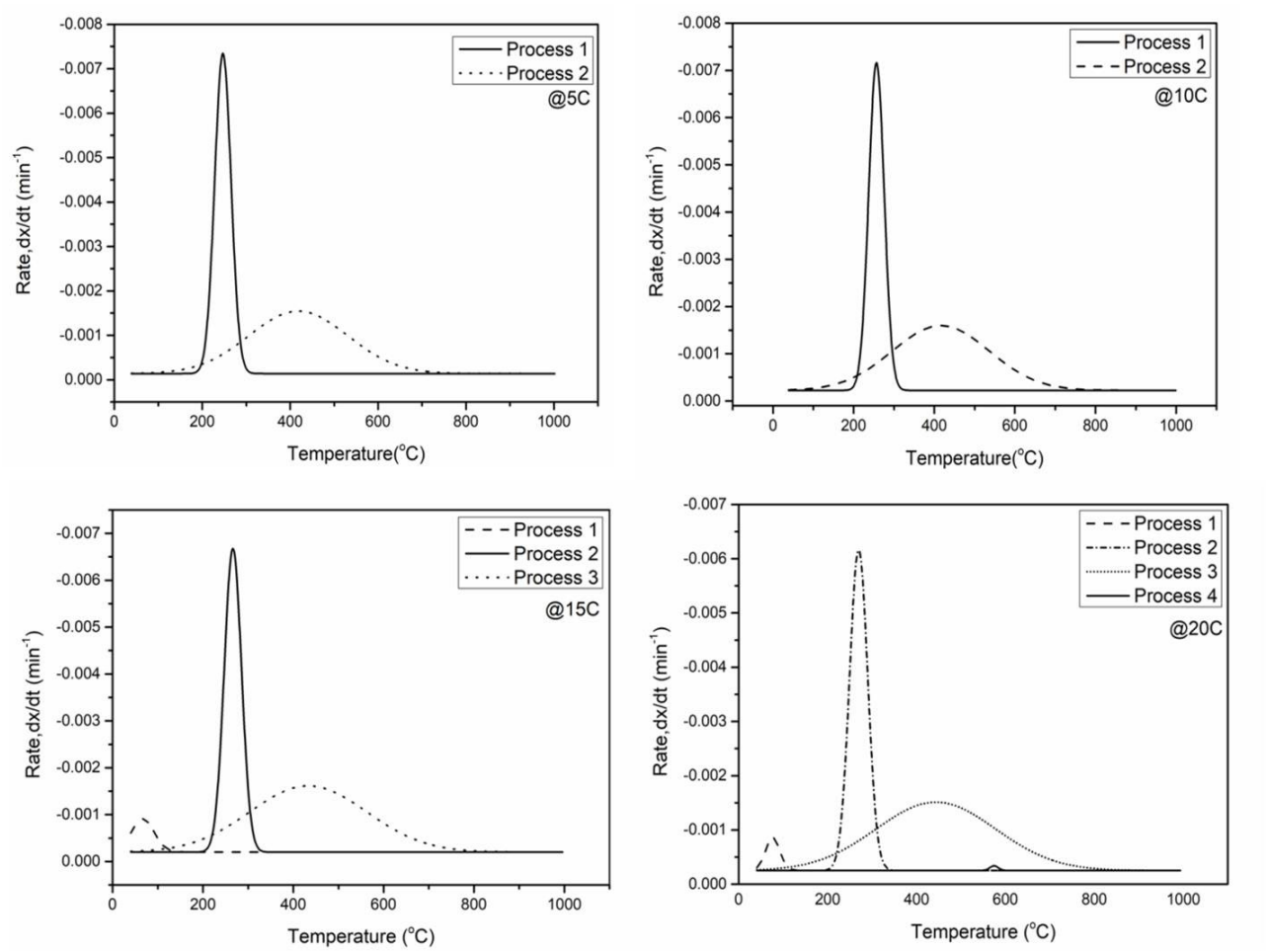

Figure 5. The procedure of deconvolution for the rate pyrolysis curve at 5, 10, 15, 20 °C min^{-1}

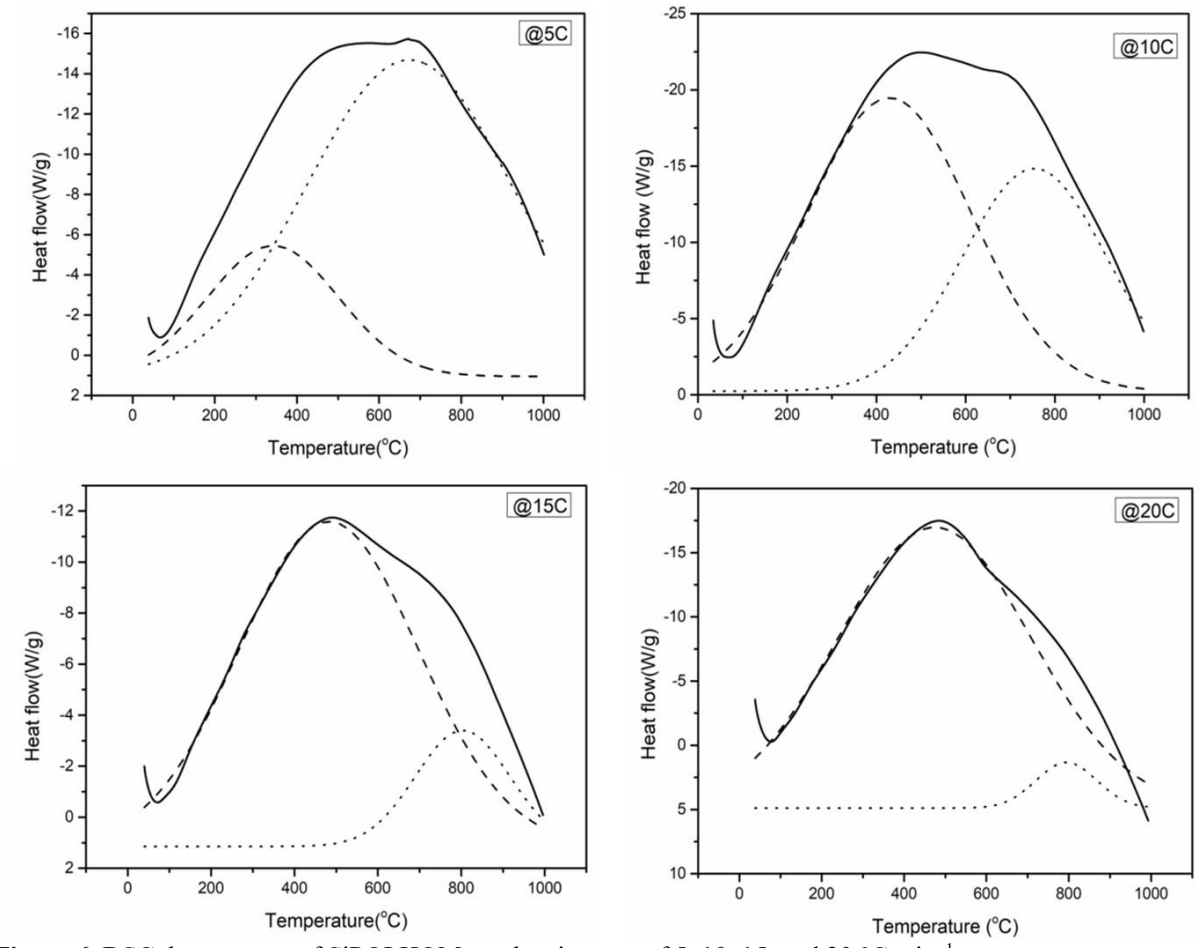

Figure 6. DSC thermogram of SiPOLHOM at a heating rate of 5, 10, 15, and 20 °C min^{-1}

Table 2. Results of deconvolution process for the degradation of SiPOLHOM

		5°C	10°C	15°C	20°C
Process 1	T_p (°C)	**246.8583**	**256.4726**	**266.22528**	**269.7015**
	$C_i \cdot [1/(2\pi)1/2 \cdot \sigma_i]$	-0.33429	-0.3325	-0.30982	-0.29949
	FWHM (°C)	43.57103	45.09463	44.90165	47.75549
	Max. Height (min^{-1})	-0.00721	-0.00693	-0.00648	-0.00589
	σ_i(°C)	43.57103	45.09463	44.90165	47.75549
Process 2	T_p (°C)	**418.3097**	**417.3487**	**432.76337**	**473.303**
	$C_i \cdot [1/(2\pi)1/2 \cdot \sigma_i]$	-0.3973	-0.50627	-0.40364	-0.56287
	FWHM (°C)	265.156	314.4975	284.67853	382.8385
	Max. Height (min^{-1})	-0.00141	-0.00151	-0.00133	-0.00138
	σ_i(°C)	265.156	314.4975	284.67853	382.8385
Process 3					**629.5319**
					0.07625
					193.7139
					3.70E-04
					193.7139
	Reduced χ^2	2.68E-08	1.91E-08	3.66E-08	1.41E-08

CONCLUSIONS

The current work deals with the kinetics of degradation of polyamidoamine (PAA) immobilized silica gel SiPOLHOM, investigated by Kissinger method and Flynn–Wall–Ozawa's (FWO) method. The apparent activation energy (Ea) was calculated by the FWO method and deconvolution method. DSC results reconfirmed the overall degradation

process constitutes two individual processes. The SiPOLHOM may be predicted as materials having potential to be applied in many fields such as adsorption, chromatography, catalysis, etc. This study is the first step towards evaluation of degradation kinetics of SiPOLHOM, keeping in view a commercial application at large scale.

REFERENCES

1. A.Ali, S. Alharthi, B. Ahmad, A. Naz, I. Khan, F. Mabood, *Molecules*, **26**(22), 6885 (2021).
2. Y. Niu, J. Yang, R. Qu, Y. Gao, N. Du, H. Chen, C. Sun, W. Wang, *Ind. Eng. Chem. Res.*, **55**, 3679 (2016).
3. S.S.Nikolića, K. V. Pavlović, M. P. Nikolić, V. V Srdić, M. Šćiban, *Mater. Res.*, 25 (2022).
4. R. K. Dey, U. Jha, T. Patnaik, A. C. Singh, V. K. Singh, *Separat. Sci. Tech.*, **44**(8), 1829 (2009).
5. R.K. Dey, T Patnaik, V.K. Singh, S.K. Swain, M A de Melo, C Airoldi, *Solid State Sci.*, **12**(4), 440 (2010).
6. V. K. Singh, S. Sur, R. Kansal, A. Kumar, P. Rathi, S. Shekhar, *Bull. Pure Appl. Sci. Chem.*, **42**(1), 27 (2023).
7. T. Nguyen, Tu. Hoai D Nguyen, T. T. T. Huynh, M-H D. Dang, L. H. T. Nguyen, T. L. H. Doan, T. P. Nguyen, M. A. Nguyen, P. H. Tran, *RSC Adv*., **12**, 19741 (2022).
8. J. A. A. Sales, G. C. Petrucelli, F.J.V.E. Oliveira, C. Airoldi, *J. Coll. Int. Sci.*, **297**(1), 95 (2006).
9. R. K. Dey, A.S. Oliveira, T. Patnaik, V. K. Singh, D. Tiwary, C. Airoldi, *J. Sold. State Chem.*, **182** (8), 2010 (2009).
10. P. Ferruti, M. A. Marchisio, R. Duncan, *Macromol. Rapid Commun.*, **23**, 332 (2002).
11. M.A. Kaczorowska, H.J. Cooper, *J. Amer. Chem. for Mass Spectr.*, **20**(4), 674 (2009).
12. R. Smaail, T. Said, E. M. Mohamed, B. Maryse, D. Stéphanie, R. Bertrand, N. M. Yahia, *J. Chem. Eng. Data*, **60**(10), 2915 (2015).
13. A. Bisht, R. Sati, K. Singhal, S. Mehtab, M.G.H. Zaidi, *Advances in Solar Power Generation and Energy Harvesting*, 127 (2020).
14. A Gamal. E.Mostafa, M. M.Hassanien, K. S. Abou-El-Sherbini, V Gorlitz, *Anal. Sci*., **19**(8), 1151 (2003).
15. S. Mehtab, A. Bisht, R. Sati, K. Singhal, S. Mehtab, M.G.H. Zaidi, *Advances in Solar Power Generation and Energy Harvesting*, 127 (2020).
16. S. Mehtab, M.G.H. Zaidi, R. Kunwar, K. Singhal, T. I. Siddiqui, *Int. J. Polym. Anal. and Charact.*, 1 (2021).
17. D. V. Quang, J. E. Lee, J. K. Kim, Y. N. Kim, G. N. Shao, H. T. Kim, *Powder Tech.*, **235**, 221 (2013).
18. K.-M. Klaudia, P. Kinga, *Polymer Composites with Functionalized Nanoparticles*, 405 (2019).
19. A. Jancirani, V. Kohila, B. Meenarathi, A.Yelilarasi, R. Anbarasan, *Bull. Mater. Sci.*, **39** (7), 1725 (2016).
20. V. Georgieva, D. Zvezdova, L. Vlaev, *Chem. Cent. J.,* 81 (2012).
21. J. B. Dahiya, K. Kumar, M. M. Hagedorn, H. Bockhorn, *Polym. Int.*, **57**(5), 722 (2008).
22. P. Joshi, G. Bisht, S. Mehtab, M.G.H. Zaidi, *Mater. Today Proc*., **62**(12), 6814 (2022).
23. S. Mehtab, M.G.H. Zaidi, N. Rana, K. Khati, S. Sharma, *Bull. Mater. Sci.*, **45**,162 (2022).
24. B. Charmas, K. Kucio, V. Sydorchuk, S. Khalameida, M. Ziezio, A. Nowicka, *Coll. Interf.*, **3**(1), 1 (2019).
25. M. Karimi, S. Davoudizadeh, S. Bahadorikhalili, K. Khezri, *Int. J. Res. Phys. Chem. Chem. Phys.,* **233**(3), 393 (2019).
26. E. Pakhmutova, Y. Slizhov, *AIP Conf. Proc*, 1899(1) (2017).
27. B. P. Jaroniec, R. K. Gilpin, M. Jaroniec, *The J. Phy. Chem. B*, **101(35)**, 6861 (1997).
28. Y. Fang, W. Yao, J. Guo, X. Gao, *Int. J.of Low-Carb. Tech.*, 7(4), 271 (2012).
29. B. Janković, *Fuel Proc. Techn.,***138**,1 (215).
30. S. Vyazovkin, *J. Thermal and Calor.,* **83**, 45 (2006).
31. L. Vlaev, N. Nedelchev, K. Gyurova, M. Zagorcheva, *J. Anal. Appl. Pyrol.,* **81**(2), 253 (2008).
32. R. K. Dey, T. Patnaik, V. K. Singh, S. K. Swain, C. Airoldi, *App. Surf. Sci.***255**(18), 8176 (2009).
33. H. E. Kissinger, *Anal. Chem.*, **29** (11), 1702 (1957).
34. P. Brachi, F. Miccio, M. Miccio, G. Ruoppolo, *Fuel Process.Tech.*,**130,** 147 (2015).
35. J. H. Flynn, L. A. Wall, *J. Res. Natl. Bur. Stand. A Phys. Chem.,* **70A** (6), 487 (1966).
36. T. Ozawa, *Thermochimica Acta*, **355**(1-2), 35 (2000).
37. J. Giuntoli, W. D. Jong, S. Arvelakis, H. Spliethoff, A. H. M. Verkooijen, *J. Anal. And Appl. Pyrol.*, **85**(1-2), 301 (2009).